Electronic Supplementary Information

Nanostructures by self-assembly of polyglycidol-derivatized lipids

Pavel Bakardzhiev, Stanislav Rangelov*, Barbara Trzebicka, Denitsa Momekova, Georgi Lalev,

Vasil M. Garamus

Synthesis and Characterization of the Precursors and Targeting DDP-Polyglycidol Polymers.

DDP-Polyglycidol polymers were prepared applying a two-step synthetic procedure presented in Fig. SI1. In the first step DDP-PEEGE precursors were prepared by ring-opening anionic polymerization of ethoxyethyl glycidyl ether (EEGE). The latter does not involve side reactions and various homo- and copolymers of good yield and molar mass distribution have been obtained.[1-6] To initiate the polymerization, partially deprotonated DDP was used. This approach provides exchange equilibrium between active chain ends and dormant, potentially active sites, which enables simultaneous growth of all chains, control of molar mass, and narrowing the dispersity. By reacting DDP with KOH and removal the released water from 50 to 80% of the hydroxyl groups were converted into alkoxide (Table SI1). A number of polymerizations were carried out aiming at preparing polymer-lipid conjugates with increasing degrees of polymerization of the polymer chain (Table SI1). It is noteworthy that all polymerizations were performed in bulk, that is, in the absence of an organic solvent. The bulk polymerization of EEGE using a macroinitiator technique has been shown to yield well-defined triblock copolymers with dispersity indices of typically below 1.20.[7-9] The GPC analysis of the DDP-PEEGE precursors gave asymmetric, not clearly resolved bimodal distributions (Fig. SI2) with dispersity of about 1.40 and higher, which was attributed to the inhomogeneity of the initiating system. The alkali metal alkoxides of DDP are solid even at temperatures as high as 90 °C, whereas the partially deprotonated DDP forms a slurry, which can hardly be uniformly distributed on the bottom of the reaction vessel. Definitely, the appearance of the initiating systems was in strong contrast with the appearance of the fluid and homogeneous macroinitiators used for the synthesis of the LGP triblock copolymers.[7-9] Measures were taken to obtain a thin film on the bottom of the reaction vessel, which was slowly dispersed upon the monomer addition. As a result the GPC curves exhibited nearly symmetric Gaussian distributions (Fig. SI3) with dispersity indices somewhat higher (1.30 – 1.35) but close to the typically observed ones for related systems.

In the second step, the protective ethoxyethyl groups of DDP-PEEGE precursors were cleaved thus yielding linear DDP-polyglycidol polymers (Scheme 1). It has recently been shown that the deprotection reaction does not cause any destruction of the polyether backbone.[7-9] The cleavage was successful as evidenced by disappearance of the signals for the methine proton at 4.6-4.7 ppm and methyl protons at 1.1-1.2 and 1.3 ppm of the acetal group in the ^{1}H NMR spectra of the resulting DDP-polyglycidol polymers (Fig. SI4). The degrees of polymerization (DPs) of both PEEGE and polyglycidol moieties were determined from the ^{1}H NMR spectra. The experimental DPs were in excellent agreement with the theoretical (targeting) DPs (Table SI1), which indicated that both the polymerizations and deprotection reactions proceeded in a controllable and predictable way.

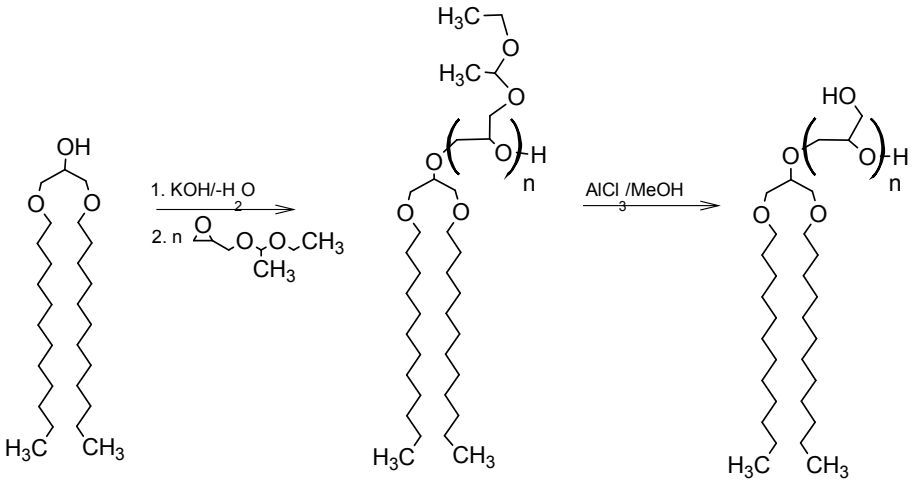

Fig. SI1 Synthesis of polyglycidol-derivatized lipids.

Table SI1 Targeting and characterization data of the DDP-polyglycidol polymers and the corresponding DDP-poly(ethoxyethyl glycidyl ether) precursors.

Targeting DP	DDP (g, mmol)	KOH (g, mmol)	EEGE (g, mmol)	Experimental DP		Abbreviation
				PEEGE	PG	
8	1.28, 2.9	0.081, 1.44	3.39, 23.0	8	8	DDP-$(G)_8$
23	0.618, 1.39	0.039, 0.69	4.7, 32.2	23	23	DDP-$(G)_{23}$
38	0.407, 0.92	0.026, 0.46	5.11, 35.0	32	30	DDP-$(G)_{30}$
55	0.535, 1.21	0.054, 0.97	9.83, 67.3	54	54	DDP-$(G)_{54}$
130	0.22, 0.5	0.022, 0.40	9.433, 64.6	110	110	DDP-$(G)_{110}$

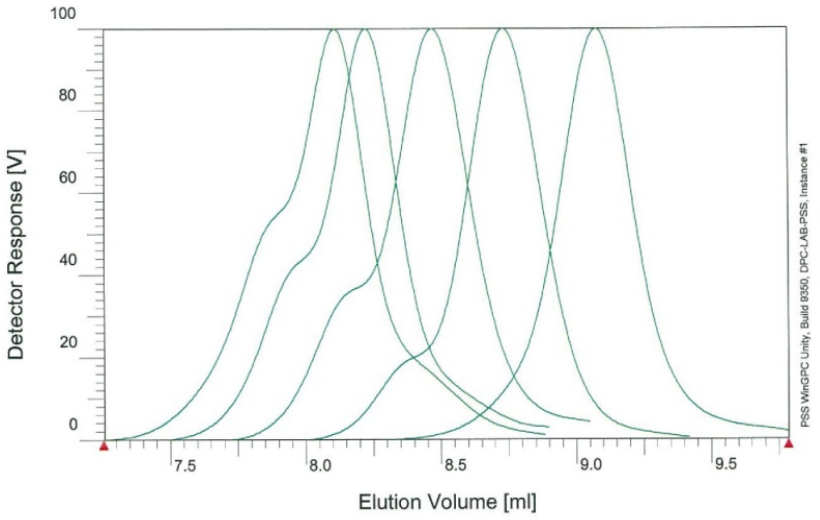

Fig. SI2 Gel permeation chromatography traces of DDP-PEEGE precursors before improvement of the initiating system preparation procedure.

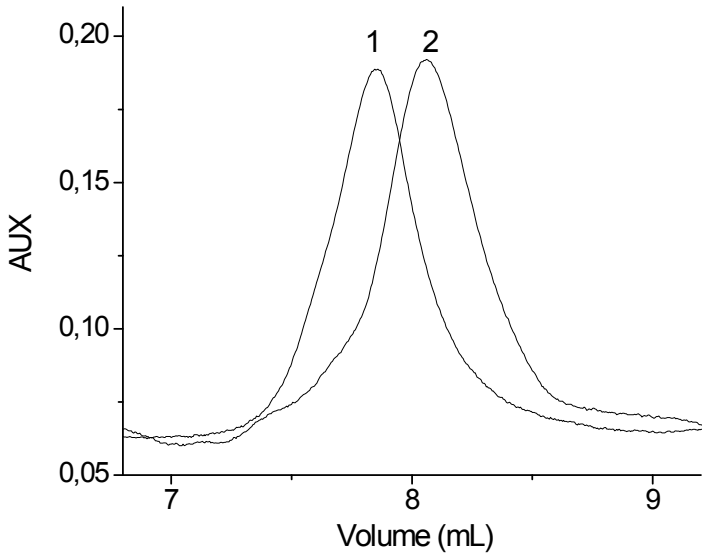

Fig. SI3 Representative gel permeation chromatography traces of DDP-$(G)_{110}$ (1) and DDP-$(G)_{54}$ (2).

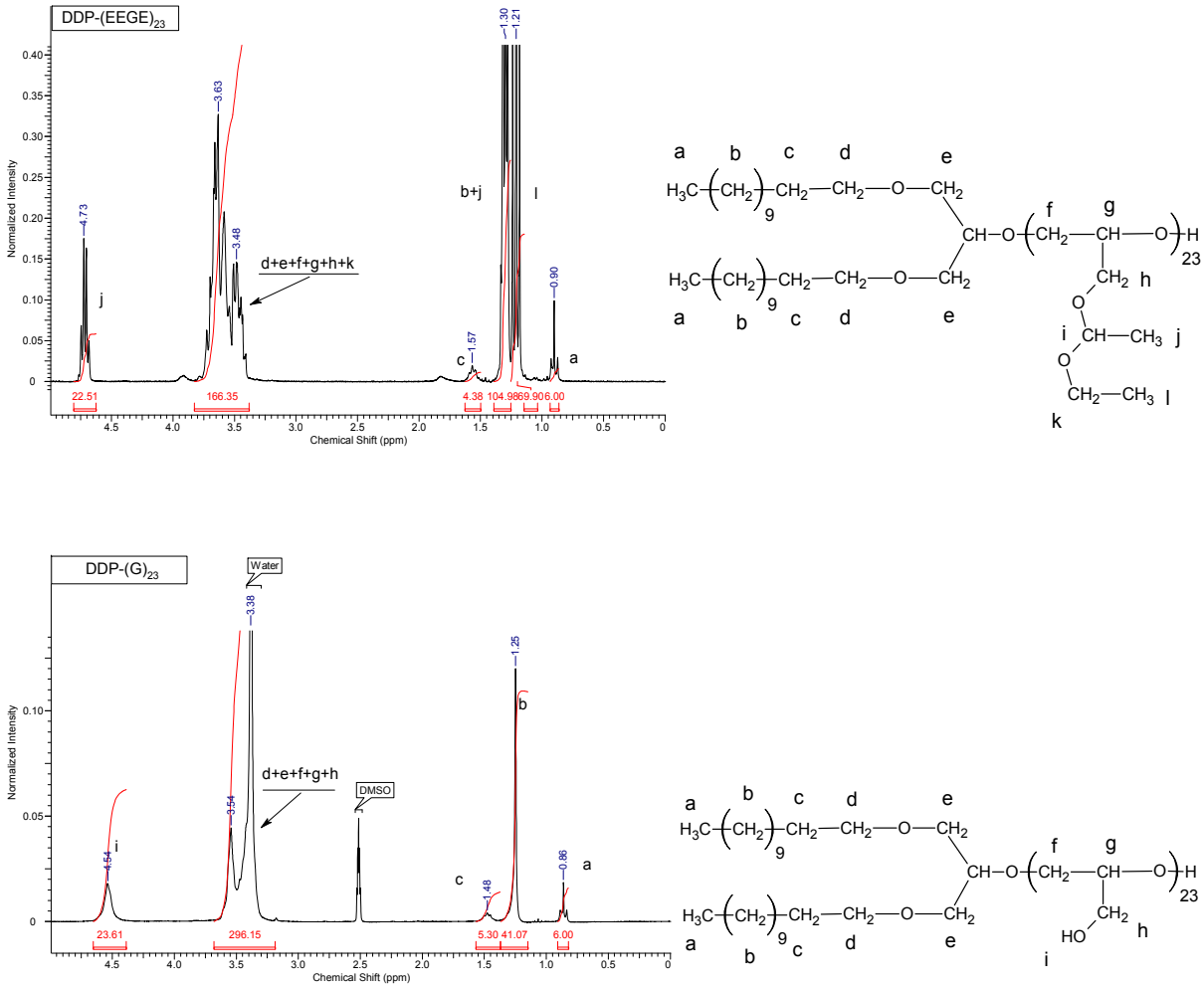

Fig. SI4 ^{1}H nuclear magnetic resonance spectra of DDP-$(EEGE)_{23}$ precursor in $CDCl_3$ (top) and the resulting DDP-$(G)_{23}$ in DMSO (bottom).

Synthetic Procedures

Preparation of the Initiator. An appropriate quantity of KOH was added to DDP magnetically stirred at 90 °C in a reaction vessel equipped with argon and vacuum lines to convert from 50 to 80% of the hydroxyl groups into alkoxide (Table SI1). After 2 h the reaction mixture was cooled to room temperature and, to remove the released water, 1 mL of dry benzene was added and vacuum was switched on for 2 h.

Polymerization (Synthesis of DDP-PEEGE precursors). EEGE (4.7 g, 32.2 mmol) was introduced to the obtained initiator to synthesize DDP-$(EEGE)_{23}$. The polymerization was carried

out in bulk at 90 °C. The conversion of the monomer was followed by ^{1}H nuclear magnetic resonance (^{1}H NMR). The syntheses of the rest of the DDP-PEEGE precursors were carried out in analogy to this procedure.

Deprotection Reaction (Synthesis of DDP−polyglycidol Polymers). The procedure was adopted from a method for deprotection of tetrahydropyranyl ether, described elsewhere.[10] 5 g of DDP-$(EEGE)_{110}$, containing 58.14 mmol of EEGE units, were dissolved in methanol (18.8 mL). $AlCl_3 \cdot 6H_2O$ (0.14 g, 0.58 mmol) was added, and the mixture was stirred for 1 h at room temperature. Afterward, the reaction product was filtered through Hylfo Super Gel (diatomaceous earth), and the solvents were evaporated under reduced pressure. The deprotection reactions for the rest of the copolymers were carried out analogously.

Aqueous Solution Properties

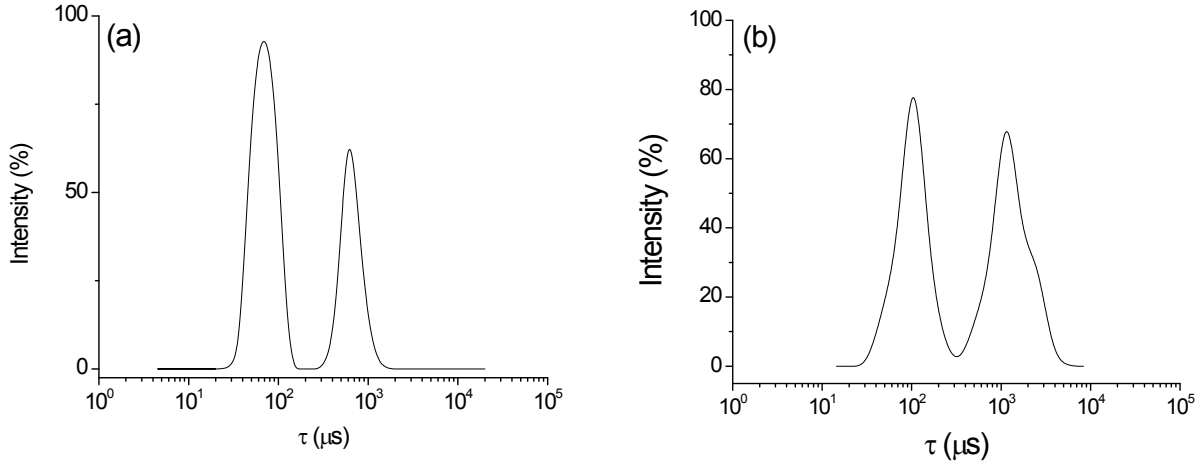

Fig. SI5 Relaxation time distributions measured at an angle of 90° and 25 °C for aqueous solutions of (a) DDP-$(G)_{30}$ and (b) DDP-$(G)_{110}$ at concentrations of 4.5 mg.mL^{-1} and 17.5 mg.mL^{-1}, respectively, before filtration.

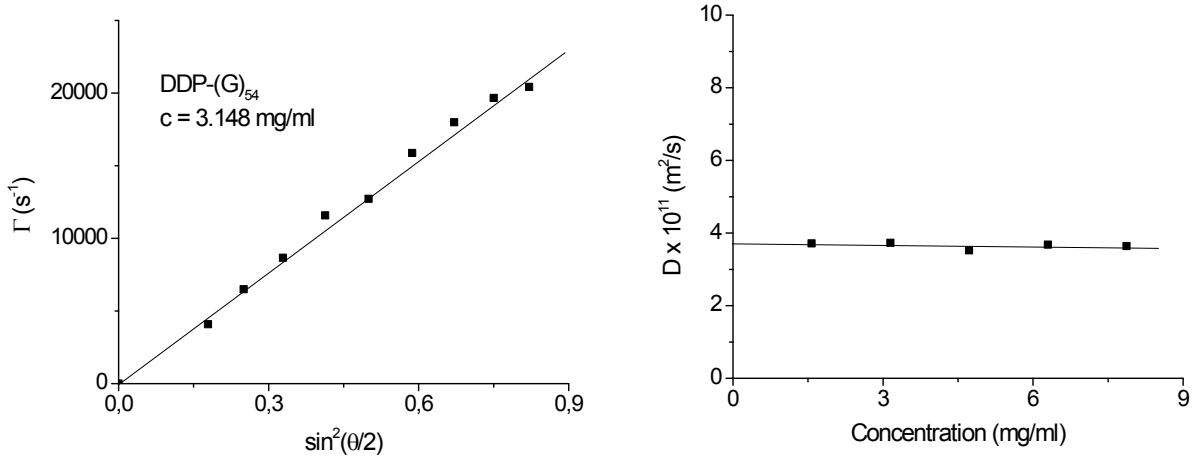

Fig. SI6 Relaxation rate (Γ) as a function of $sin^2(\theta/2)$ for DDP-$(G)_{54}$ in water at c = 3.148 mg.mL^{-1} and 25 °C (left). Concentration dependence of the diffusion coefficients for DDP-$(G)_{54}$ (right). The lines through the data points represent the linear fits to the data.

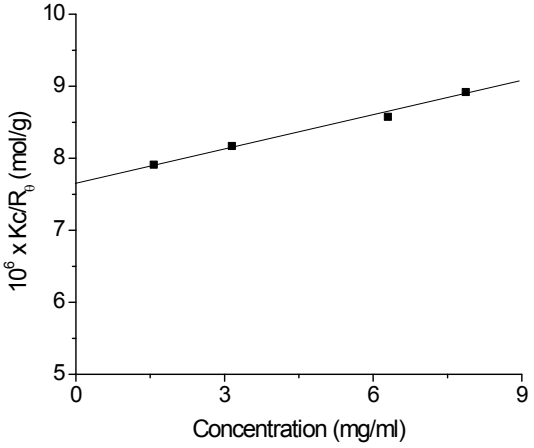

Fig. SI7 Reduced scattered light intensity measured at an angle of 90°, Kc/R_{90}, as a function of concentration of DDP-$(G)_{54}$ at 25 °C. The lines through the data points represent the linear fits to the data.

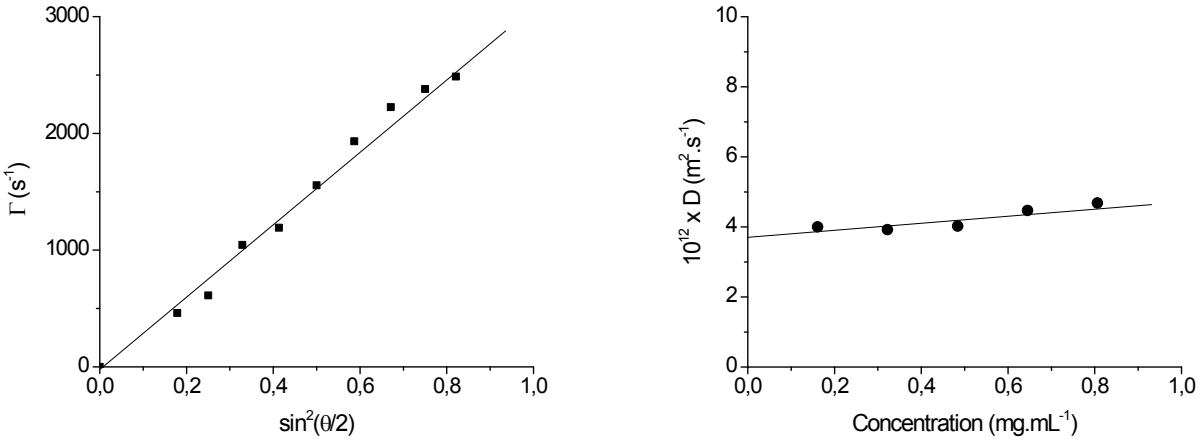

Fig. SI8 Relaxation rate (Γ) as a function of $sin^2(\theta/2)$ for DDP-$(G)_8$ in water at c = 0.806 mg.mL^{-1} and 25 °C (left). Concentration dependence of the diffusion coefficients for DDP-$(G)_8$ (right). The lines through the data points represent the linear fits to the data.

Small-Angle X-ray Scattering (SAXS) Study

The aqueous dispersions of DDP-$(G)_8$ were studied by SAXS. The downward curvature of the scattering intensities at q < 0.015 Å^{-1} indicates repulsive interactions between the objects. Therefore, the data at q > 0.015 Å^{-1} (here the effect of the interactions on the scattering curves is negligible) were analyzed by the indirect Fourier transformation (IFT) method with the approximation of infinitely thin non-interactive objects.[11] The scattering intensities for disk-like aggregates were written in the form of the thickness pair distance distribution function $p_T(r)$:

$$d\Sigma(q)/d\Omega = (\frac{2\pi}{q^2})\pi\int_0^\infty p_T(r)\cos(qr)dr \qquad \text{(Eq. 1)}$$

The $p_T(r)$ function is given as:[12]

$$p_T(r) = \frac{c}{2\pi M_S}\int \Delta\rho(r')\Delta\rho(r+r')dr' \qquad \text{(Eq. 2)},$$

where r is the coordinate in the x-direction, M_S corresponds to the mass per surface unit of disk-like aggregates, $\Delta\rho(r)$ is the scattering contrast at point r of the object $\Delta\rho(r) = \rho(r) - \rho_s$, $\rho(r)$ is the scattering length density at point r, and ρ_s is the average scattering length density of solvent.

Negative values of $p_T(r)$ at intermediate r indicate that the scattering contrasts for the hydrocarbon chains and the hydrophilic polyglycidol chains in aqueous solution are of different signs, *i.e.*, positive for the alkyl groups and negative for polyglycidol. If density of 1 g.mL^{-1} for

all constituents is assumed, scattering length densities of $9.7 \cdot 10^{10}$ cm^{-2}, $9.2 \cdot 10^{10}$ cm^{-2} and $9.4 \cdot 10^{10}$ cm^{-2} for CH_2 (alkyl), $C_3H_6O_2$ (polyglycidol) and water, respectively, can be estimated.

$p_T(r)$ function was further deconvoluted to get profiles of scattering contrast within the layer[12] (Fig. SI9). It is seen that the change from a positive contrast (alkyl chain region) to a negative contrast (polyglycidol) takes place at r ~ 10 Å and the thickness of the polyglycidol region is ~ 15 Å. Assuming a sandwich-like structure of the membrane, composed of an inner hydrocarbon layer and two outer polyglycidol layers, it was possible to estimate the thicknesses of the sublayers. The quantities that were obtained were 21 Å for the hydrocarbon chain layer and 16 – 18 Å for each of the two outer layers.

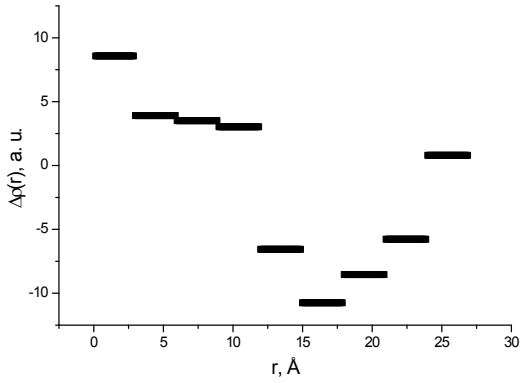

Fig. SI9 Profile of the scattering contrast from the center of the bilayer.

References

1 D. Taton, A. Le Borgne, M. Sepulchre and N. Spassky, *Macromol. Chem. Phys.* 1994, **195**, 139-48.
2 A. Dworak, I. Panchev, B. Trzebicka and W. Walach, *Macromol. Symp.* 2000, **153**, 233-42.
3 A. Dworak, G. Baran, B. Trzebicka and W. Walach, *React. Funct. Polym.* 1999, **42**, 31-6.
4 W. Walach, B. Trzebicka, J. Jystynska and A. Dworak, *Polymer* 2004, **45**, 1755-62.
5 Ph. Dimitrov, S. Rangelov, A. Dworak and Ch. Tsvetanov, *Macromolecules* 2004, **37**, 1000-8.
6 Ph. Dimitrov, S. Rangelov, A. Dworak, N. Haraguchi, A. Hirao and Ch. Tsvetanov, *Macromol. Symp.* 2004, **215**, 127-40.
7 S. Halacheva, S. Rangelov and Ch. Tsvetanov, *Macromolecules* 2006, **39**, 6845-52.
8 S. Halacheva, S. Rangelov and Ch. Tsvetanov, *Macromolecules* 2008, **41**, 7699-705.
9 S. Halacheva, S. Rangelov, Ch. Tsvetanov and V. M. Garamus, *Macromolecules* 2010, **43**, 772-81
10 V. V. Namboodri and R. S. Varma, *Tetrahedron Lett.* 2002, **43**, 1143-6.
11 O. Glatter, *J. Appl. Cryst.* 1977, **10**, 415-421.

12 J. S. Pedersen, *Adv. Colloid Interf. Sci.* 1997, **70**, 171-210.